Large Increase in Incident Shortwave Radiation due to the Ozone Hole Offset by High Climatological Albedo over Antarctica

G. CHIODO

Department of Applied Physics and Applied Mathematics, Columbia University, New York, New York

L. M. POLVANI

Department of Applied Physics and Applied Mathematics, Department of Earth and Environmental Sciences, and Lamont-Doherty Earth Observatory, Columbia University, New York, New York

M. PREVIDI

Lamont-Doherty Earth Observatory, Columbia University, New York, New York

(Manuscript received 28 November 2016, in final form 22 February 2017)

ABSTRACT

Despite increasing scientific scrutiny in recent years, the direct impact of the ozone hole on surface temperatures over Antarctica remains uncertain. Here, this question is explored by using the Community Earth System Model–Whole Atmosphere Community Climate Model (CESM-WACCM), contrasting two ensembles of runs with and without stratospheric ozone depletion. It is found that, during austral spring, the ozone hole leads to a surprisingly large increase in surface downwelling shortwave (SW) radiation over Antarctica of 3.8 W m^{-2} in clear sky and 1.8 W m^{-2} in all sky. However, despite this large increase in incident SW radiation, no ozone-induced surface warming is seen in the model. It is shown that the lack of a surface temperature response is due to reflection of most of the increased downward SW, resulting in an insignificant change to the net SW radiative heating. To first order, this reflection is simply due to the high climatological surface albedo of the Antarctic snow (97% in visible SW), resulting in a net zero ozone-induced surface SW forcing. In addition, it is shown that stratospheric ozone depletion has a negligible effect on longwave (LW) radiation and other components of the surface energy budget. These results suggest a minimal role for ozone depletion in forcing Antarctic surface temperature trends on a continental scale.

1. Introduction

Among the climatic effects of stratospheric ozone depletion in the Southern Hemisphere (SH) [see Previdi and Polvani (2014) for a comprehensive review], the most evident include the large cooling (8 K) of the Antarctic lower stratosphere during spring (Randel et al. 2009) and delayed breakup of the stratospheric polar vortex (Waugh et al. 1999). Observations in the SH also show a positive trend in the southern annular mode (SAM) in summertime (Marshall 2003), which is associated with a poleward shift of the midlatitude jet (Archer and Caldeira 2008), and poleward expansion of the Hadley cell (Min and Son 2013). There is robust modeling evidence pointing to a dominant role for ozone depletion in driving these trends (Gillett and Thompson 2003; Polvani et al. 2011; Min and Son 2013). However, while the effects of the ozone hole on atmospheric circulation in the middle to low latitudes of the SH are well established, its influences on Antarctic surface climate remain poorly understood.

Observed Antarctic surface temperature trends over recent decades show a distinct warming of the Antarctic Peninsula and of West Antarctica (Turner et al. 2005; Monaghan et al. 2008; Steig et al. 2009). In contrast, slight cooling trends have been reported over East Antarctica (Schneider et al. 2012). It has been suggested that stratospheric ozone depletion could have contributed to the spatial structure of these trends through changes in the SAM (Thompson and Solomon 2002; Gillett and Thompson 2003; Schneider et al. 2012). However, the largest SAM trends in recent decades are found in the summer, whereas the largest Antarctic temperature trends occur in different seasons (Smith

Corresponding author: G. Chiodo, chiodo@columbia.edu

DOI: 10.1175/JCLI-D-16-0842.1

and Polvani 2017). An alternative, and as yet unexplored, pathway whereby the ozone hole could affect Antarctic surface temperatures is through direct forcing of the surface energy budget.

Idealized modeling studies have shown that a decrease in stratospheric ozone concentration has a large impact on radiative forcing (RF) at the tropopause, with opposite effects on shortwave (SW) and longwave (LW) fluxes (Ramanathan and Dickinson 1979; Ramaswamy et al. 1992; Conley et al. 2013; Myhre et al. 2013). The annual mean, global mean RF associated with stratospheric ozone depletion is quite small, on the order of $-0.05\,\mathrm{W\,m^{-2}}$ [cf. Conley et al. (2013), their Table 2]. However, the RF can locally be much larger, such as over Antarctica during austral spring [cf. Myhre et al. (2013), their Fig. 8.23]. The ozone hole effects on surface climate could not be investigated in those studies because of either the simplicity of the models employed (Ramanathan and Dickinson 1979; Ramaswamy et al. 1992) or the fixed tropospheric temperatures used in standard RF calculations (Conley et al. 2013; Myhre et al. 2013).

Here, using ensembles of simulations from a coupled atmosphere–ocean climate model with interactive ozone photochemistry (CESM-WACCM), we quantify in detail the impact of ozone depletion on the Antarctic surface energy budget. We show that the ozone hole leads to a sizable late-twentieth-century increase in incident (downward) SW radiation on the Antarctic surface. However, despite this large SW perturbation, the modeled Antarctic surface temperature does not increase significantly. This lack of a surface temperature response is shown to be due to the high climatological snow albedo over Antarctica, which reflects the increased incident SW flux, thus leading to negligible net surface RF.

2. Methods

We employ the Community Earth System Model (CESM) with the atmospheric component being the stratosphere-resolving Whole Atmosphere Community Climate Model, version 4 (WACCM4) (Marsh et al. 2013). WACCM4 has a horizontal resolution of 1.9° latitude by 2.5° longitude, with 66 vertical levels, extending up to 140 km, and realistically simulates the chemical effects of ozone-depleting substances (ODSs) on stratospheric ozone (Marsh et al. 2013). Additionally, WACCM is coupled to the Parallel Ocean Program (POP) (Gent et al. 2011), and to the Community Land Model version 4 (CLM4) (Lawrence et al. 2011), which incorporates parameterizations for several snow and ice processes, such as grain-size-dependent snow aging.

To quantify the impact of twentieth-century ozone depletion on Antarctic surface climate, we contrast two CESM-WACCM ensembles, each comprising six integrations for the period 1960 to 2005 (see also Marsh et al. 2013; Smith et al. 2013). For the reference ensemble (labeled "HIST"), all natural and anthropogenic forcings are specified as in CMIP5 (phase 5 of the Coupled Model Intercomparison Project) historical integrations, with individual ensemble members initialized from these CMIP5 integrations. The second ensemble (labeled "fixODS") is identical to HIST except for the prescribed surface concentrations of ODSs, which are kept constant at year 1955 levels. Therefore, HIST includes the ODS-induced stratospheric ozone depletion during the twentieth century, while fixODS does not. The focus will be on the late austral spring [October–December (OND)], which is the season when stratospheric ozone depletion maximizes, and when the strongest surface RF is therefore expected.

3. Results

The evolution of springtime (OND) total ozone, averaged over the Antarctic continent, is shown in Fig. 1a. In the HIST ensemble, half of the ozone column is depleted by the year 1990, as compared to the fixODS ensemble in which there are no discernible ozone trends. The climatological ozone column in WACCM4 is a little low, but the total ozone loss simulated in the historical ensemble [140 Dobson units (DU)] is in good agreement with Michelson Interferometer for Passive Atmospheric Sounding (MIPAS) satellite data (Peck et al. 2015).

Accompanying this large stratospheric ozone depletion, one sees a large increase in clear-sky downwelling SW radiation at the Antarctic surface in the HIST ensemble (Fig. 2a). After clouds are taken into account ("all-sky"), this increase in SW radiation is reduced, especially over West Antarctica (Fig. 2b). The partial compensation by clouds is best seen by comparing the SW flux changes in visible and UV ($\lambda < 750\,\mathrm{nm}$) (Fig. 2c) with changes in the near-infrared ($750\,\mathrm{nm} < \lambda < 1500\,\mathrm{nm}$) (Fig. 2d). The large increase in the broadband integrated SW flux ($3.8\,\mathrm{W\,m^{-2}}$) displayed in Fig. 2a lies entirely in the visible and UV range (Fig. 2c).

However, an increase in cloud cover over West Antarctica in HIST partly reduces the incident near-infrared SW flux at the surface (Fig. 2d), owing to enhanced cloud absorption (Zender et al. 1997). A simple regression analysis reveals that the SAM accounts for approximately 30% of the cloud trends (not shown). However, the significance of the correlation between the SAM and the cloud fraction over western Antarctica is low ($p < 0.1$), and the ensemble spread is large.

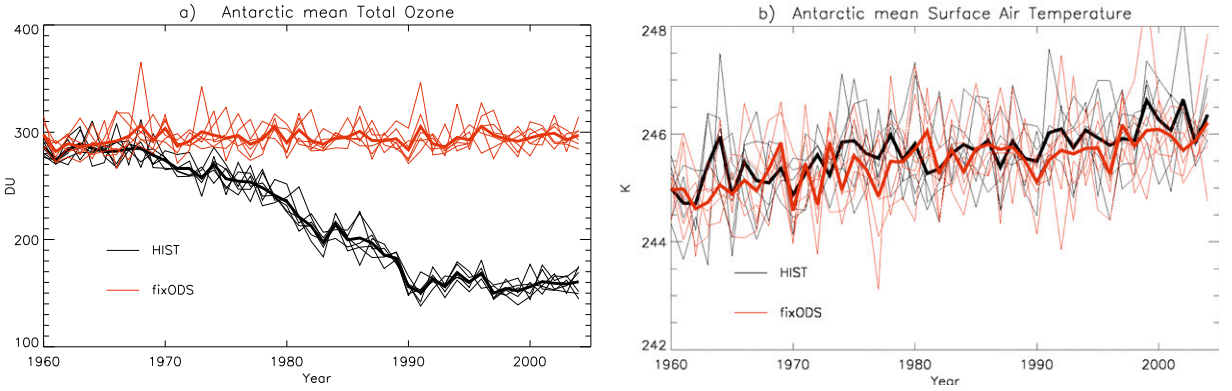

FIG. 1. (a) Time series of Antarctic mean total column ozone values in spring (OND) in Dobson units (DU). Thin lines indicate the six individual ensemble members, while thick lines show the ensemble average (red for fixODS and black for HIST). (b) As in (a), but for surface air temperature, in K.

Moreover, the reduction in near-infrared is smaller than the increase in at shorter wavelengths. As a result, the overall SW flux change integrated over all wavelengths (Fig. 2b) is significant over most of the continent, and is on average $+1.8\,\mathrm{W\,m^{-2}}$. Additional offline calculations using the Parallel Offline Radiative Transfer (PORT) model (Conley et al. 2013) reveal that the increase in clear-sky downwelling SW radiation in HIST is directly linked to the decrease in stratospheric ozone concentrations (not shown).

One might question whether the simulated ozone-induced changes in SW radiation are realistic, given the relatively coarse spectral resolution of the solar radiation scheme in WACCM4. To investigate this, we have performed single-column clear-sky calculations with the line-by-line libRadtran model (Mayer and Kylling 2005), using total column ozone values corresponding to the 1990–2005 Antarctic average for the fixODS and HIST ensembles simulated by WACCM4 (i.e., 300 DU and 160 DU) and a zenith angle of 80° (representative of Antarctic conditions in spring). The resulting downwelling clear-sky broadband integrated SW spectral irradiance is shown in Fig. 3. In response to the imposed ozone depletion, we find an enhanced SW flux of $3.61\,\mathrm{W\,m^{-2}}$ (i.e., the area between the black and the red curves), in good agreement with the WACCM4 model output ($3.4\,\mathrm{W\,m^{-2}}$; see Fig. 2c). The libRadtran calculations reveal that the contribution from the UV range (250–350 nm) is relatively small ($0.37\,\mathrm{W\,m^{-2}}$), and that the bulk of the incident SW increase ($3.01\,\mathrm{W\,m^{-2}}$) is produced at visible wavelengths (500–650 nm), where a peak in ozone absorptivity is located (see the dashed green line in Fig. 3), known as the Chappuis band (Anderson and Mauersberger 1992). The UV absorption band quickly saturates, while Chappuis absorption band is in the weak-line limit, approximately linear in the path length [cf. Lacis and Hansen (1974), their Fig. 6]. For this reason, Chappuis is the dominant absorption band at the large solar zenith angles that characterize Antarctic conditions. From this, we conclude that the sizable OND increase in incident SW flux induced by the ozone hole shown in Fig. 2 is a realistic feature.[1]

In spite of the large SW perturbation, both WACCM ensembles show a similar warming trend in Antarctic mean surface temperature in spring (Fig. 1b), as well as in other seasons (not shown). The lack of an enhanced surface warming in the presence of the ozone hole implies the existence of a mechanism that opposes the increased downward SW flux. To determine this mechanism, we first carefully examine the surface energy balance.

For both the HIST and fixODS ensembles, we calculate the spring (OND) changes between the pre- (1960–75) and post- (1990–2005) ozone hole periods, for each of the terms in the surface energy budget. Over this period, changes in energy storage are negligible, due to the presence of dry snow with low heat conductivity, such that surface temperature adjusts rapidly to changes in the surface energy budget (Trenberth 1983; van den Broeke et al. 2004). Contrasting the red (fixODS) and black (HIST) symbols in Fig. 4, one sees that the ozone hole has no influence on turbulent energy exchange, or on downwelling and upwelling LW radiation.[2] Unlike

[1] Despite the large intraseasonal variability in incident SW and ozone column values, an ozone-induced increase in clear-sky SW radiation in WACCM can be detected in daily data throughout OND, indicating that 3-month OND averages are representative.

[2] Note that the lack of a surface LW change with ozone depletion is in contrast to what occurs at the tropopause, where the net LW forcing from ozone depletion is negative (see, e.g., Ramanathan and Dickinson 1979; Ramaswamy et al. 1992; Conley et al. 2013): this suggests that the Antarctic troposphere is opaque to LW changes originating in the stratosphere despite the small water vapor abundances.

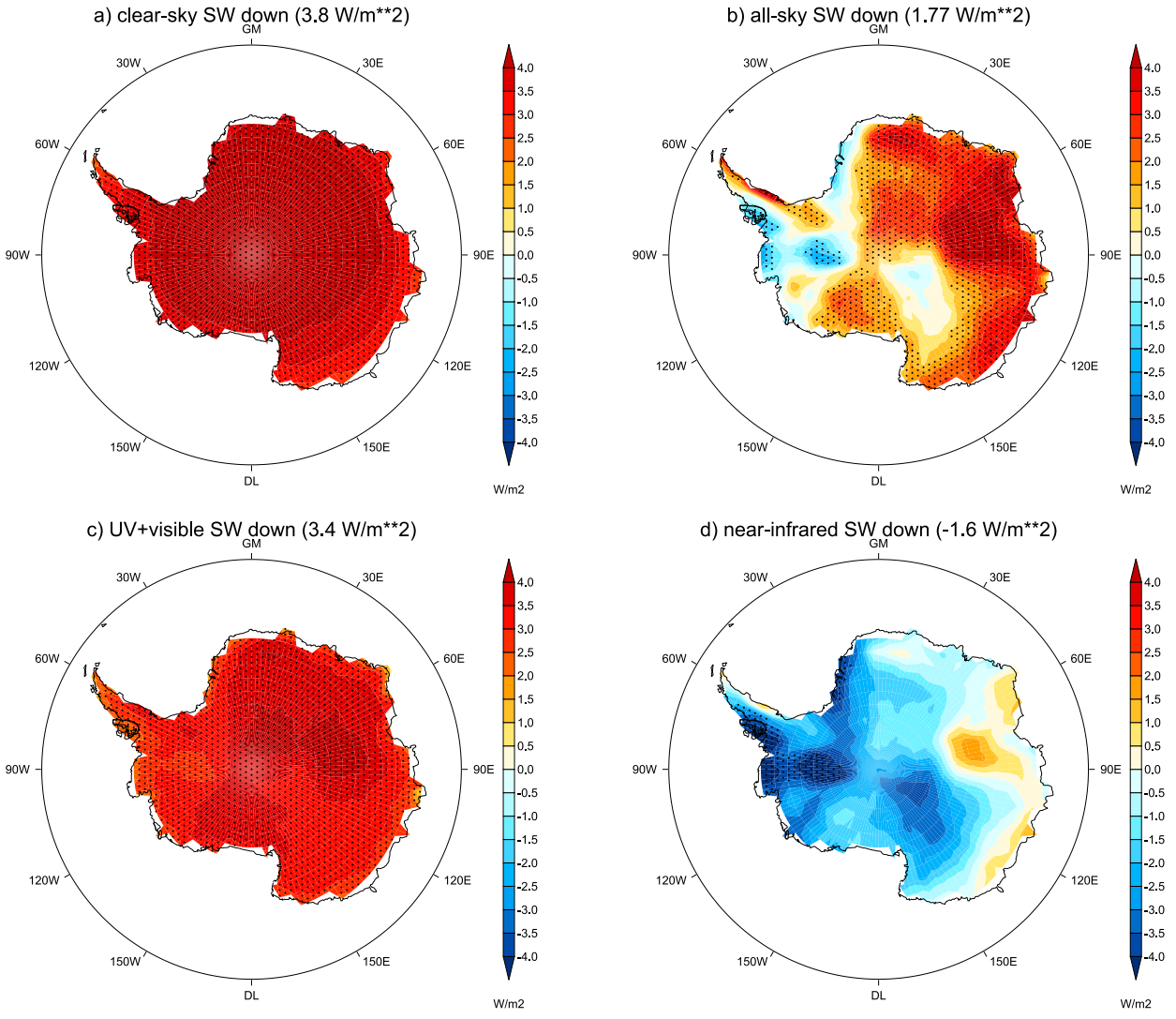

FIG. 2. (a) Ensemble-mean difference (HIST − fixODS) over the 1990–2005 period in springtime (OND) downwelling (incident) clear-sky SW radiation flux at the surface. Stippling denotes statistical significance. (b) As in (a), but for all-sky downward SW flux at the surface. (c) As in (a), but for the all-sky downward UV plus visible ($250 < \lambda < 750$ nm) SW flux. (d) As in (c), but for the near-infrared ($750 < \lambda < 1500$ nm) SW flux. Values in parentheses indicate the Antarctic area-weighted average. Units are $W\,m^{-2}$.

the LW, a clear separation between the two ensembles is apparent in the SW surface clear-sky downward flux, with an increase in this flux of about $3\,W\,m^{-2}$ in the HIST and a decrease of $1\,W\,m^{-2}$ in the fixODS ensembles, respectively. The increase in clear-sky SW radiation in HIST is also in good agreement with the libRadtran and PORT calculations (blue and green symbols). Note that this increase in clear-sky SW radiation in the HIST ensemble is of the same magnitude as the simulated increase over the 1960–2005 period in downward surface LW radiation associated with greenhouse gases (GHGs) ($3–5\,W\,m^{-2}$; see Fig. 4).

Note, furthermore, that the opposite-signed long-term changes in surface downwelling SW radiation in the two ensembles are due to the opposing effects: the GHGs induced moistening (which decreases the SW↓ flux) and the ozone hole itself (which increases the SW↓ flux). The clear-sky difference in the downwelling SW flux between the two ensembles is partly reduced in all-sky conditions, due to an increase in total cloud cover in the HIST ensemble (see Fig. 2b). Most importantly, the increase in downward SW radiation in HIST, under both clear-sky and all-sky conditions, is approximately balanced by an increase in the upward SW flux (SW↑) (i.e., the SW↑ component in HIST is within the ensemble spread of the SW↓ component), leaving a very small change in the net absorbed surface SW radiation (SWn).

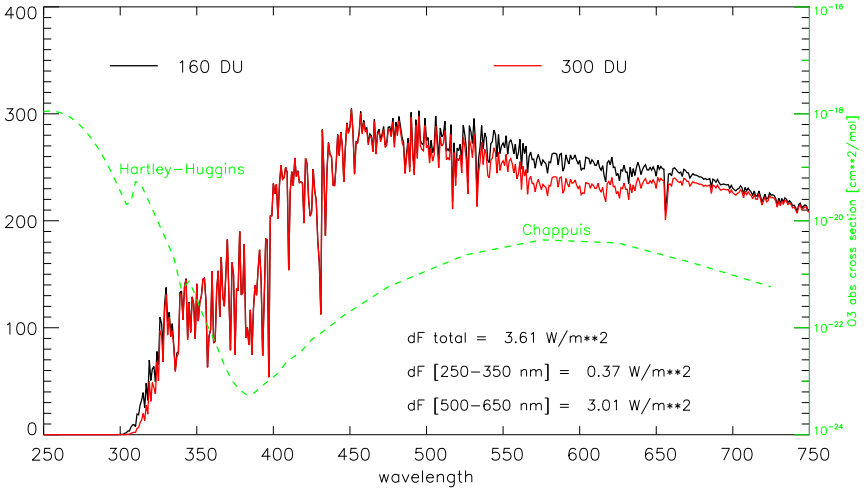

FIG. 3. Downwelling clear-sky SW spectral irradiance at the surface, as calculated by the libRadtran line-by-line code using the Antarctic total column ozone values from the HIST (black) and fixODS (red) ensembles, and a zenith angle of 80. dF is the integrated area between the two curves. The green line depicts the absorption cross section of ozone as parameterized in WACCM4.

To elucidate the origin of the increase in upward SW flux (and thus of the lack of surface temperature changes), we analyze the surface albedo computed by the land component of CESM-WACCM (CLM4) over Antarctica, which is shown in Fig. 5a for visible and UV, and in Fig. 5b for near-infrared bands. In WACCM, the mean climatological albedo in the visible and UV is 0.97, while it is 0.69 in the near-infrared. These values are consistent with the microphysical properties of Antarctic snow, as derived from modeling (Wiscombe and Warren 1980) and observational campaigns (Grenfell et al. 1994). Since the ozone-induced SW flux changes are produced almost entirely in the highly reflective visible range (Fig. 3), nearly all (97%) of the increase in

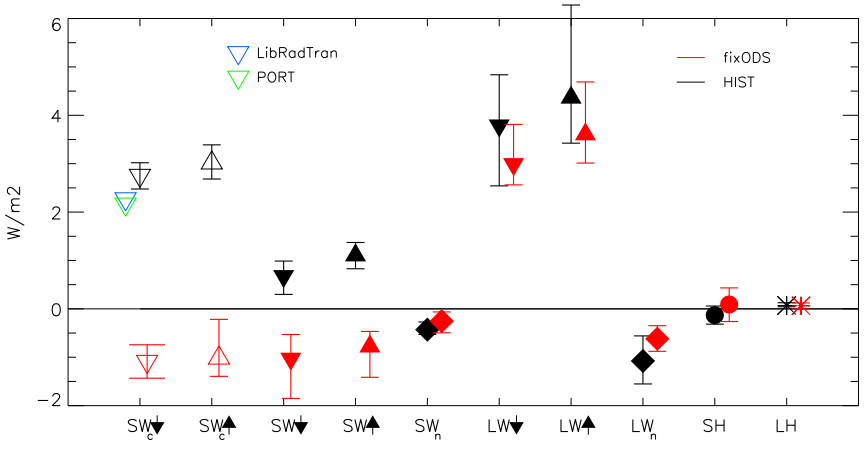

FIG. 4. Post- (1990–2005) minus pre- (1960–1975) ozone hole climatological difference in springtime (OND) Antarctic mean surface energy budget terms. The *c* subscript stands for clear sky. The arrows identify the direction of the SW and LW fluxes, and the *n* subscript denotes net fluxes. Each symbol represents the ensemble mean, with black and red symbols denoting the HIST and fixODS ensembles, and the uncertainty bars representing the ensemble spread. The blue and green symbols represent the change (with respect to the fixODS ensemble mean) in clear-sky SW radiation, as calculated in the LbL libRadtran and offline PORT radiative transfer models, respectively. Units are W m^{-2}.

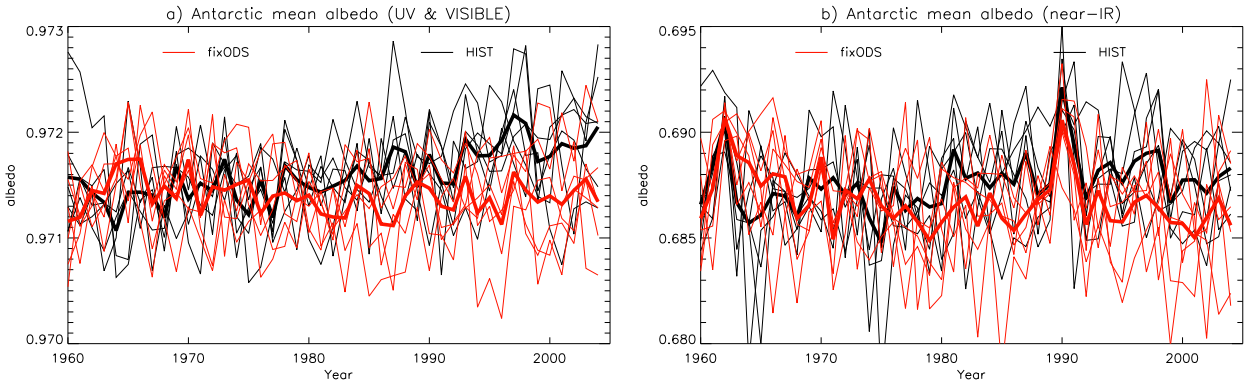

FIG. 5. Time series of springtime Antarctic mean surface albedo in the (a) visible/UV ($250 < \lambda < 750$ nm), and (b) near-infrared ($750 < \lambda < 1500$ nm) bands. Thin lines indicate the six individual ensemble members, while thick lines show the ensemble average (red for fixODS and black for HIST).

the broadband integrated upward SW (SW↑ in Fig. 4) is due to the increase in the downward SW flux, which is simply reflected: this is the familiar ''albedo'' effect of the Antarctic surface.

Thus, of the 3.4 W m^{-2} increase in UV/visible downwelling radiation in HIST with respect to the fixODS ensemble (Fig. 2c), the albedo effect alone cancels 3.3 W m^{-2}. We also find a small positive trend in the UV/visible albedo in the HIST ensemble (Fig. 5a). This corresponds to a small but significant upward trend of 0.1% (0.971 to 0.972). In Fig. 5b, we also see that over the 1990–2005 period, the albedo in HIST appears to be higher (by 0.001) than in fixODS in the near-infrared (750 nm $< \lambda <$ 1500 nm), but the differences between the two ensembles in this spectral range are not statistically significant.

The contribution of these albedo changes between HIST and fixODS to the increase in upward SW irradiance in HIST (see SW↑ in Fig. 4) can be quantified by scaling the OND average incident SW radiation in the HIST ensemble (179.5 W m^{-2}) by the broadband albedo difference between HIST and fixODS (0.002): this yields $179.5 \times 0.002 \approx 0.3$ W m^{-2}, which explains why the ensemble mean SW↑ in HIST is slightly larger (by 0.3–0.4 W m^{-2}) than SW↓. Note, however, that the upwelling and downwelling SW flux increases in HIST are statistically indistinguishable, since the error bars in SW↑ and SW↓ overlap. Thus, the lack of an ozone-induced warming is overwhelmingly due to the high climatological albedo in the UV/visible range, with the albedo trends playing a very minor role.

Observational records of radiative fluxes would be highly valuable to validate the model results presented in this work. However, high-quality station data of SW and LW radiation over Antarctica only extend back to the early 1990s (Frederick and Hodge 2011) and thus do not encompass the period of rapid springtime polar ozone loss in the 1970s and 1980s (e.g., see Fig. 1a). It is worth noting, though, that the continental broadband average albedo in WACCM (0.82) is close to the values obtained from remote sensing (Laine 2008). In addition, direct measurements support the notion that Antarctic snow albedo is very high in the spectral bands where ozone has the largest effect (Grenfell et al. 1994; Flanner and Zender 2006). Hence, ozone depletion has little potential for radiatively influencing the Antarctic surface energy budget.

4. Conclusions

We have investigated the impact of springtime stratospheric ozone depletion on the Antarctic surface temperature. The main results are as follows:

- The ozone hole leads to a considerable increase (3.8 W m^{-2}) in downward surface SW radiation over the Antarctic continent (in OND). Offline calculations with a line-by-line radiative transfer model suggest that the ozone-induced increase in downwelling surface SW radiation in WACCM is realistic, and is due to reduced stratospheric absorption in the Hartley–Huggins (250–350 nm) and Chappuis (550–600 nm) ozone bands, with the latter playing a dominant role.
- Despite the large ozone-hole-induced increase in the downward SW flux, there is little change in the net SW absorption at the Antarctic surface. This is primarily due to the high albedo of Antarctic snow in the spectral bands where ozone has a large effect. The high albedo inhibits any direct radiative effect of the ozone hole at the Antarctic surface.

Changes in the surface downwelling LW radiation associated with ozone depletion could potentially have a

much greater effect on Antarctic surface temperature, given the high absorptivity of Antarctic snow at these wavelengths (Tedesco 2014) [cf. Warren (1982), their Fig. 18a]. However, these LW changes are small compared to the ozone-induced SW perturbations (Fig. 4): this explains the minimal role for ozone depletion in forcing surface temperature trends on a continental scale (Fig. 1b). Finally, we note that even though our results are based on a single model, they are likely to be robust across models with realistic Antarctic albedo. On the other hand, the albedo trends that are simulated in WACCM (Fig. 5a) may depend on the snow aging scheme, and are therefore likely to be model dependent. Further work is needed to elucidate this aspect.

Acknowledgments. We thank Stephen Warren for his constructive comments, which helped improve the quality of the paper. This work is supported by the U.S. NSF Frontiers of Earth System Dynamics award to Columbia University. All model integrations were performed at the National Center for Atmospheric Research (NCAR), which is sponsored by the U.S. National Science Foundation. All the simulation data can be obtained by request to author GC.

REFERENCES

Anderson, S. M., and K. Mauersberger, 1992: Laser measurements of ozone absorption cross sections in the Chappuis band. *Geophys. Res. Lett.*, **19**, 933–936, doi:10.1029/92GL00780.

Archer, C. L., and K. Caldeira, 2008: Historical trends in the jet streams. *Geophys. Res. Lett.*, **35**, L08803, doi:10.1029/2008GL033614.

Conley, A., J. Lamarque, F. Vitt, W. Collins, and J. Kiehl, 2013: PORT, a CESM tool for the diagnosis of radiative forcing. *Geosci. Model Dev.*, **6**, 469–476, doi:10.5194/gmdd-5-2687-2012.

Flanner, M. G., and C. S. Zender, 2006: Linking snowpack microphysics and albedo evolution. *J. Geophys. Res.*, **111**, D12208, doi:10.1029/2005JD006834.

Frederick, J., and A. Hodge, 2011: Solar irradiance at the Earth's surface: Long-term behavior observed at the South Pole. *Atmos. Chem. Phys.*, **11**, 1177–1189, doi:10.5194/acp-11-1177-2011.

Gent, P. R., and Coauthors, 2011: The Community Climate System Model version 4. *J. Climate*, **24**, 4973–4991, doi:10.1175/2011JCLI4083.1.

Gillett, N. P., and D. W. Thompson, 2003: Simulation of recent Southern Hemisphere climate change. *Science*, **302**, 273–275, doi:10.1126/science.1087440.

Grenfell, T. C., S. G. Warren, and P. C. Mullen, 1994: Reflection of solar radiation by the Antarctic snow surface at ultraviolet, visible, and near-infrared wavelengths. *J. Geophys. Res.*, **99**, 18 669–18 684, doi:10.1029/94JD01484.

Lacis, A., and J. Hansen, 1974: A parameterization for the absorption of solar radiation in the Earth's atmosphere. *J. Atmos. Sci.*, **31**, 118–133, doi:10.1175/1520-0469(1974)031<0118:APFTAO>2.0.CO;2.

Laine, V., 2008: Antarctic ice sheet and sea ice regional albedo and temperature change, 1981–2000, from AVHRR Polar Pathfinder data. *Remote Sens. Environ.*, **112**, 646–667, doi:10.1016/j.rse.2007.06.005.

Lawrence, D. M., and Coauthors, 2011: Parameterization improvements and functional and structural advances in version 4 of the Community Land Model. *J. Adv. Model. Earth Syst.*, **3**, M03001, doi:10.1029/2011MS00045.

Marsh, D. R., M. J. Mills, D. E. Kinnison, J.-F. Lamarque, N. Calvo, and L. M. Polvani, 2013: Climate change from 1850 to 2005 simulated in CESM1 (WACCM). *J. Climate*, **26**, 7372–7391, doi:10.1175/JCLI-D-12-00558.1.

Marshall, G. J., 2003: Trends in the southern annular mode from observations and reanalyses. *J. Climate*, **16**, 4134–4143, doi:10.1175/1520-0442(2003)016<4134:TITSAM>2.0.CO;2.

Mayer, B., and A. Kylling, 2005: Technical note: The libRadtran software package for radiative transfer calculations—Description and examples of use. *Atmos. Chem. Phys.*, **5**, 1855–1877, doi:10.5194/acp-5-1855-2005.

Min, S.-K., and S.-W. Son, 2013: Multimodel attribution of the Southern Hemisphere Hadley cell widening: Major role of ozone depletion. *J. Geophys. Res. Atmos.*, **118**, 3007–3015, doi:10.1002/jgrd.50232.

Monaghan, A. J., D. H. Bromwich, W. Chapman, and J. C. Comiso, 2008: Recent variability and trends of Antarctic near-surface temperature. *J. Geophys. Res.*, **113**, D04105, doi:10.1029/2007JD009094.

Myhre, G., and Coauthors, 2013: Anthropogenic and natural radiative forcing. *Climate Change 2013: The Physical Science Basis*, T. Stocker et al., Eds., Cambridge University Press, 659–740.

Peck, E., C. Randall, V. Harvey, and D. Marsh, 2015: Simulated solar cycle effects on the middle atmosphere: WACCM3 versus WACCM4. *J. Adv. Model. Earth Syst.*, **7**, 806–822, doi:10.1002/2014MS000387.

Polvani, L. M., D. W. Waugh, G. J. Correa, and S.-W. Son, 2011: Stratospheric ozone depletion: The main driver of twentieth-century atmospheric circulation changes in the Southern Hemisphere. *J. Climate*, **24**, 795–812, doi:10.1175/2010JCLI3772.1.

Previdi, M., and L. M. Polvani, 2014: Climate system response to stratospheric ozone depletion and recovery. *Quart. J. Roy. Meteor. Soc.*, **140**, 2401–2419, doi:10.1002/qj.2330.

Ramanathan, V., and R. E. Dickinson, 1979: The role of stratospheric ozone in the zonal and seasonal radiative energy balance of the Earth–troposphere system. *J. Atmos. Sci.*, **36**, 1084–1104, doi:10.1175/1520-0469(1979)036<1084:TROSOI>2.0.CO;2.

Ramaswamy, V., M. Schwarzkopf, and K. Shine, 1992: Radiative forcing of climate from halocarbon-induced global stratospheric ozone loss. *Nature*, **355**, 810–812, doi:10.1038/355810a0.

Randel, W. J., and Coauthors, 2009: An update of observed stratospheric temperature trends. *J. Geophys. Res.*, **114**, D02107, doi:10.1029/2008JD010421.

Schneider, D. P., C. Deser, and Y. Okumura, 2012: An assessment and interpretation of the observed warming of west Antarctica in the austral spring. *Climate Dyn.*, **38**, 323–347, doi:10.1007/s00382-010-0985-x.

Smith, K. L., and L. M. Polvani, 2017: Spatial patterns of recent Antarctic surface temperature trends and the importance of natural variability: Lessons from multiple reconstructions and the CMIP5 models. *Climate Dyn.*, **48**, 2653–2670, doi:10.1007/s00382-016-3230-4.

——, M. Previdi, and L. M. Polvani, 2013: The Antarctic atmospheric energy budget. Part II: The effect of ozone depletion and its projected recovery. *J. Climate*, **26**, 9729–9744, doi:10.1175/JCLI-D-13-00173.1.

Steig, E. J., D. P. Schneider, S. D. Rutherford, M. E. Mann, J. C. Comiso, and D. T. Shindell, 2009: Warming of the Antarctic ice-sheet surface since the 1957 International Geophysical Year. *Nature*, **457**, 459–462, doi:10.1038/nature07669.

Tedesco, M., 2014: *Remote Sensing of the Cryosphere.* John Wiley & Sons, 432 pp.

Thompson, D. W., and S. Solomon, 2002: Interpretation of recent Southern Hemisphere climate change. *Science*, **296**, 895–899, doi:10.1126/science.1069270.

Trenberth, K. E., 1983: What are the seasons? *Bull. Amer. Meteor. Soc.*, **64**, 1276–1282, doi:10.1175/1520-0477(1983)064<1276:WATS>2.0.CO;2.

Turner, J., and Coauthors, 2005: Antarctic climate change during the last 50 years. *Int. J. Climatol.*, **25**, 279–294, doi:10.1002/joc.1130.

van den Broeke, M., C. Reijmer, and R. van de Wal, 2004: Surface radiation balance in Antarctica as measured with automatic weather stations. *J. Geophys. Res.*, **109**, D09103, doi:10.1029/2003JD004394.

Warren, S. G., 1982: Optical properties of snow. *Rev. Geophys.*, **20**, 67–89, doi:10.1029/RG020i001p00067.

Waugh, D. W., W. J. Randel, S. Pawson, P. A. Newman, and E. R. Nash, 1999: Persistence of the lower stratospheric polar vortices. *J. Geophys. Res.*, **104**, 27 191–27 201, doi:10.1029/1999JD900795.

Wiscombe, W. J., and S. G. Warren, 1980: A model for the spectral albedo of snow. I: Pure snow. *J. Atmos. Sci.*, **37**, 2712–2733, doi:10.1175/1520-0469(1980)037<2712:AMFTSA>2.0.CO;2.

Zender, C., and Coauthors, 1997: Atmospheric absorption during the Atmospheric Radiation Measurement (ARM) Enhanced Shortwave Experiment (ARESE). *J. Geophys. Res.*, **102**, 29 901–29 915, doi:10.1029/97JD01781.